Active Particles Powered by Quincke Rotation in a Bulk Fluid

Debasish Das[*] and Eric Lauga[†]

Department of Applied Mathematics and Theoretical Physics, Centre for Mathematical Sciences,
University of Cambridge, Wilberforce Road, Cambridge CB3 0WA, United Kingdom

Dielectric particles suspended in a weakly conducting fluid are known to spontaneously start rotating under the action of a sufficiently strong uniform dc electric field due to the Quincke rotation instability. This rotation can be converted into translation when the particles are placed near a surface providing useful model systems for active matter. Using a combination of numerical simulations and theoretical modeling, we demonstrate that it is possible to convert this spontaneous Quincke rotation into spontaneous translation in a plane perpendicular to the electric field in the absence of surfaces by relying on geometrical asymmetry instead.

How are groups of living organisms such as flocks of birds, schools of fish and bacterial colonies able to self-organize and display collective motion [1]? This question has fascinated scientists for decades and has given rise to the new field of "active matter" [2,3]. One of the key features of active matter is that it is composed of self-propelled units that move by consuming energy from their surrounding with a direction of self-propulsion typically set by their own anisotropy, either in shape or functionalization, rather than by an external field.

The origin of macroscopic ordered motion in active systems is due to microscopic interactions occurring at an individual level. Ideally, one would like to develop a coarse-grained description of active systems from these microscopic interactions but these are difficult to measure or quantify, forcing scientists to develop phenomenological models [4,5]. "Nonliving" active systems offer a simplified and more controlled setting compared to "living" active systems, and there have been multiple attempts to design self-propelled synthetic particles in the laboratory [6]. Examples include bimetallic Janus particles powered by catalytic reactions [7,8], electric [9,10] and magnetic field driven colloids [11], light activated colloidal surfers [12], water droplets driven by Marangoni stress [13], and self-propelled squirming droplets [14].

In recent active matter experiments, it has been possible to measure and quantify these microscopic interactions [9,10]. These experiments consisted of spherical colloids able to roll along surfaces by exploiting the so-called Quincke rotation, discovered more than a century ago [15]. The Quincke phenomenon involves the application of a uniform electric field that gives rise to the spontaneous rotation of dielectric solid particles or deformable drops suspended in a slightly conducting fluid medium [16–18]. Quincke rotation is best explained using the much celebrated Melcher-Taylor leaky dielectric model [19] that

proposes the formation of a surface charge on the particle-liquid interface. Rotation occurs due to the symmetry breaking of the charge distribution that gives rise to a net torque leading to steady rotation of the particle.

There are two conditions for Quincke rotation to occur. First, the charge relaxation time of the particle, τ^-, must exceed that of the surrounding fluid, τ^+, where $\tau^\pm = \epsilon^\pm/\sigma^\pm$ with $\epsilon^\pm$ and $\sigma^\pm$ being the permittivity and conductivity, respectively (superscript $-$ representing particle and $+$ representing fluid). This implies that the particle must be less conducting than the surrounding fluid, giving rise to a dipole moment, $\boldsymbol{P}$, which is antiparallel to the applied electric field, $\boldsymbol{E}_0$. This configuration is unstable and the electric torque, $\boldsymbol{T}_E \propto \boldsymbol{P} \times \boldsymbol{E}_0$, tends to rotate the particle away from its original orientation. The second condition requires that the magnitude of the electric field exceeds a critical value, E_C, for sustained rotation of the particle, $E_0 > E_C$, such that the electric torque balances the viscous torque.

In an infinite fluid medium, a symmetric particle such as a sphere under Quincke rotation will steadily rotate without translating as no net external force acts on it. This spontaneous rotation can be converted into spontaneous translation when the particle is placed near a wall. Such "Quincke rollers" were demonstrated experimentally to perform collective motion due to electrohydrodynamic interactions with each other and with the nearby surface [9,10].

In this Letter, we show that it is possible to convert spontaneous Quincke rotation into spontaneous translation in the absence of surfaces. Specifically, asymmetrically shaped dielectric particles placed in the bulk of a slightly conducting fluid will spontaneously acquire both rotation and translation under the action of a sufficiently strong uniform dc electric field in a plane perpendicular to the field. We demonstrate this phenomenon by focusing on the

electrohydrodynamics of a helix—an archetypal chiral particle—first computationally, using the boundary element method, and then by developing an analytical theory in quantitative agreement with the simulations.

Consider an uncharged neutrally buoyant solid particle of volume, V^-, surface, S, and outward unit normal vector, n, suspended in an infinite fluid medium of volume, V^+ (see Fig. 1). The dynamic viscosity of the fluid is denoted by μ. The particle gets polarized due to the application of a uniform dc electric field, $E_0 = E_0 \hat{z}$. We define two dimensionless numbers $R = \sigma^+/\sigma^-$ and $Q = \varepsilon^-/\varepsilon^+$ such that $RQ = \tau^-/\tau^+ > 1$ is the necessary condition for Quincke rotation to take place. In the Melcher-Taylor leaky dielectric model, all charges are concentrated on the particle surface, so that the electric potential in each domain satisfies Laplace's equation $\nabla^2 \varphi^\pm = 0$ [19]. All the physical quantities are implicitly assumed to be a function of time. On the particle surface, the electric potential and the tangential component of the local electric field are continuous $[\![\varphi(x)]\!] = 0$ and $[\![E_t(x)]\!] = 0$ for $x \in S$, where $E_t^\pm = (I - nn)\cdot E^\pm$, $E^\pm = -\nabla \varphi^\pm$ and $[\![f(x)]\!] \equiv f^+(x) - f^-(x)$ denotes the jump for any field variable $f(x)$ defined on both sides of the particle surface. The normal component of the electric field $E_n^\pm = n\cdot E^\pm$ undergoes a jump due to the mismatch in electrical properties between the two media [20], resulting in a surface charge distribution given by Gauss's law, $q(x) = [\![\varepsilon E_n(x)]\!]$ for $x \in S$. The surface charge distribution evolves due to two distinct mechanisms, namely, Ohmic currents from the bulk, $[\![\sigma E_n]\!]$, and advection by the particle surface velocity, $v(x)$. Accordingly, the conservation equation for the surface charge is

$$\partial_t q + [\![\sigma E_n]\!] + \nabla_s \cdot (q v) = 0 \quad \text{for } x \in S, \qquad (1)$$

where $\nabla_s \equiv (I - nn)\cdot \nabla$ is the surface gradient operator. The fluid velocity field, $v(x)$, and dynamic pressure, $p(x)$, satisfy the Stokes equations in the suspending fluid, $-\mu \nabla^2 v + \nabla p = 0$ and $\nabla \cdot v = 0$. No slip at the solid-fluid interface leads to kinematic boundary conditions for the
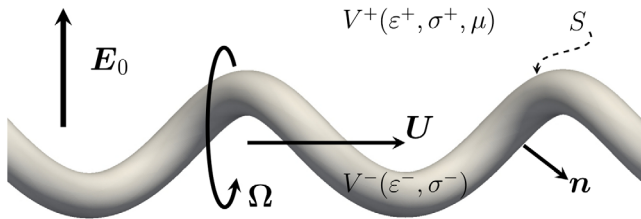

FIG. 1. Schematic representation of the problem considered in this Letter. A solid particle of volume V^-, surface S, and outward unit normal vector n is suspended in an infinite fluid of volume V^+ and subject to a uniform dc electric field, $E_0 = E_0 \hat{z}$. The electric permittivities and conductivities of the suspending fluid and particle are denoted as ε^+, σ^+ and ε^-, σ^-, respectively, and the dynamic viscosity of the fluid is μ. The translational and angular velocity of the particle are U and Ω, respectively.

fluid velocity, $v(x) = U + \Omega \times (x - x_c)$ for $x \in S$, where U, Ω, and x_c are the translational velocity, rotational velocity, and centroid of the particle. In the absence of inertia, the dynamic balance of electric and hydrodynamic forces and torques on the solid particle requires $F_E + F_H = 0$ and $T_E + T_H = 0$, respectively. The forces and torques are found by integrating the surface tractions f

$$F_{E,H} = \oint_S f_{E,H} dS(x), \qquad (2)$$

$$T_{E,H} = \oint_S (x - x_c) \times f_{E,H} dS(x). \qquad (3)$$

The electric and hydrodynamic tractions are expressed in terms of the Maxwell stress tensor, T_E, and hydrodynamic stress tensor, T_H, respectively as

$$f_E = n\cdot T_E = n\cdot \left[\varepsilon \left(EE - \frac{1}{2}E^2 I \right) \right], \qquad (4)$$

$$f_H = n\cdot T_H = n\cdot [-pI + \mu(\nabla v + \nabla v^T)]. \qquad (5)$$

To demonstrate that it is possible to convert Quincke rotation into spontaneous translation without the need for any surfaces, we consider a dielectric filament of helical shape in an infinite fluid. Helices are prototypical chiral particles used to create synthetic swimmers [21,22], and their propulsive abilities at low Reynolds number flows have been well characterized in the context of bacterial locomotion [23]. The centerline of the helix is specified as $r(\xi) = \xi \hat{x} + R_h \cos(2\pi \chi \xi/\lambda)\hat{y} + R_h \sin(2\pi \chi \xi/\lambda)\hat{z}$ using parameter $\xi \in [-L_\lambda, L_\lambda]$, where $L_\lambda = N\lambda$ is the axial length, λ is the helical pitch, N is the number of turns, and R_h is the helical radius. The arc and contour length of the helix are $s = \xi/\cos\alpha$ and $L = L_\lambda/\cos\alpha$, respectively, where $\alpha = \arctan(2\pi R_h/\lambda)$ is the pitch angle. The cross section of the helical filament is denoted as a. Here, $\chi = \pm 1$ determines the chirality of the helix and we focus on right-handed helices, $\chi = 1$, without any loss of generality.

We use the boundary element method to solve the electrohydrodynamics of a cylindrical and helical particle [24,25] (see the Supplemental Material [26] for details). We show in Figs. 2(a)–2(d) snapshots of a cylinder and a helix having identical aspect ratio (i.e., the cylinder can be obtained by simply uncoiling the helix) moving under the action of an external uniform DC electric field. We specify the dimensionless electric field strength, $E^* = E_0/E_{C,cl}$, where the critical electric field for Quincke rotation of a cylinder is $E_{C,cl} = [2\mu/\varepsilon^+ \tau_{\mathrm{MW},cl}(\bar{\varepsilon}_{cl} - \bar{\sigma}_{cl})]^{1/2}$ with $\bar{\varepsilon}_{cl} = (\varepsilon^- - \varepsilon^+)/(\varepsilon^- + \varepsilon^+)$ and $\bar{\sigma}_{cl} = (\sigma^- - \sigma^+)/(\sigma^- + \sigma^+)$ [32]. Time is nondimensionalized with the characteristic Maxwell-Wagner timescale for polarization of a cylindrical particle upon the application of an electric field, $\tau_{\mathrm{MW},cl} = (\varepsilon^- + \varepsilon^+)/(\sigma^- + \sigma^+)$. The axes of both rigid
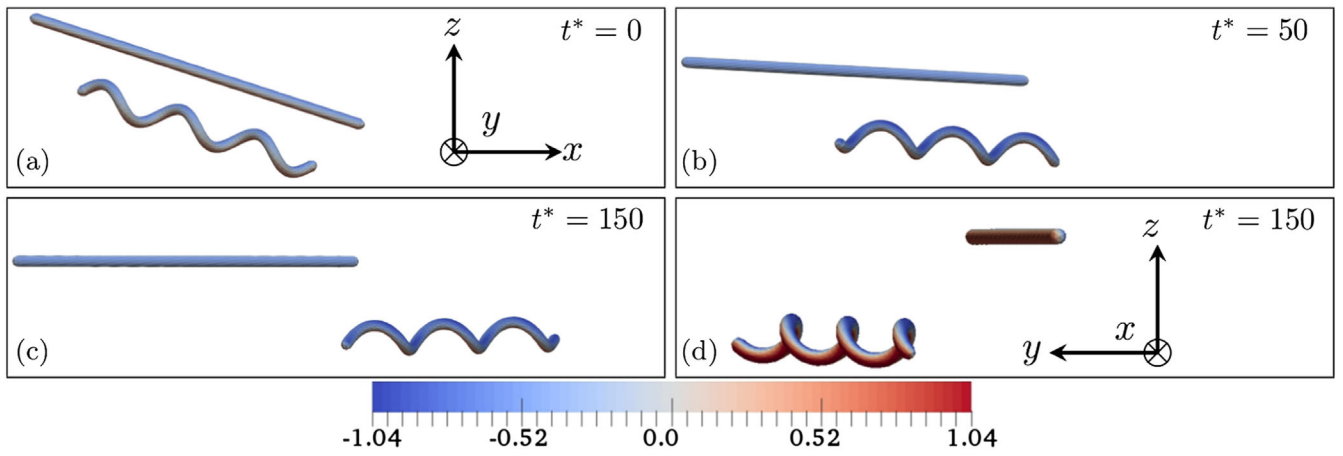
FIG. 2.   (a)–(c) Snapshots of a cylinder and a helix having an aspect ratio of $a/L = 0.0167$ under Quincke rotation due to an applied electric field $\boldsymbol{E}_0^* = 2.5\hat{\boldsymbol{z}}$ with $R = Q = 2$. The helix has $N = 3$ turns, pitch angle $\alpha = 0.2\pi$, and pitch $\lambda/L = 0.236$. The particles are slightly tilted with respect to the x axis at an angle 0.1π at time $t^* = 0$. The cylinder performs pure rotation while the helix undergoes rotation as well as translation perpendicular to the z axis. (d) Rotated view of snapshot (c) showing the positively charged side of the particles. The particles move out of the $x-z$ plane due to their initially tilted configuration. The colorbar indicates surface charge distribution. Associated movies are available in the Supplemental Material [26].

particles are initially tilted at an angle of 0.1π with respect to the x axis in the $x-z$ plane. Because the applied electric field, $\boldsymbol{E}_0^* = E_0^*\hat{\boldsymbol{z}}$, is higher than the critical field for both particles, they spontaneously start rotating. The directions of rotation for both particles are always perpendicular to the electric field, i.e., $\boldsymbol{\Omega}\cdot\boldsymbol{E}_0 = 0$ [26], and thus both align their axes in a direction perpendicular to the electric field in the steady state. As predicted by theory, the cylinder undergoes pure rotation with no translation. In contrast, the asymmetric shape of the helix allows it to undergo both rotation and translation. Furthermore, we plot the net displacement of the cylinder (cl) and helix (hl) in three dimensions in time; see Fig. 3. Note that the particles move out of the $x-z$ plane due to their initially tilted configuration.

In contrast to Quincke rollers, the helical particle in Fig. 2 undergoes spontaneous translation in the absence of surfaces, and thus represents a new type of active self-propelling particle in bulk fluids. In order to further probe
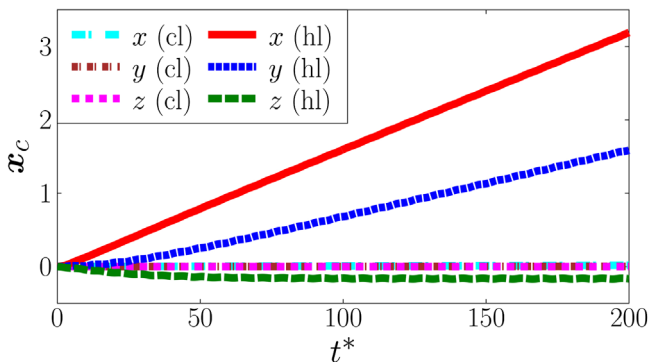

FIG. 3.   Three-dimensional trajectories of the centroid of the cylinder (cl) and the helix (hl).

its ability to swim, we investigate in Fig. 4 how its steady swimming speed, U, depends on various geometrical parameters (numerical data are shown in symbols while the lines represent the theory developed below). First, we show in Fig. 4(a) how the magnitude of the critical electric field depends on the pitch angle, α, for various cross-sectional radii, a/λ, with fixed number of turns. The critical field required to generate rotation of the helix is seen to systematically increase above its value for a cylinder as the amplitude of the helix grows and as the filament becomes more slender.

Next we plot in Fig. 4(b), the value of the steady swimming speed, U, as a function of the helix pitch angle, α, for two different electric field strengths while keeping the cross-sectional radius fixed. The swimming speed is zero for a straight rod ($\alpha = 0$) and a torus ($\alpha = \pi/2$) and thus is maximal when the pitch angle takes an intermediate value, $\alpha \approx 0.2\pi$ (simulations) and 0.215π (theory) for $E^* = 2.5$ and $\alpha \approx 0.25\pi$ (simulations and theory) for $E^* = 5.5$. Finally, the effect of the aspect ratio of the helix, a/L, on the swimming speed, U, is shown in Fig. 4(c) keeping other geometrical quantities fixed. The swimming speed undergoes a supercritical pitchfork bifurcation so that swimming does not occur for a/L below a critical value (i.e., for particles that are too slender).

The computational results obtained above can be rationalized using theoretical arguments. The hydrodynamic forces and torques acting on a helix are linearly related to its translation and angular velocities through the 6×6 resistance matrix $\boldsymbol{R}$ as

$$\begin{pmatrix} \boldsymbol{F}_H \\ \boldsymbol{T}_H \end{pmatrix} = -\boldsymbol{R}\cdot\begin{pmatrix} \boldsymbol{U} \\ \boldsymbol{\Omega} \end{pmatrix}. \tag{6}$$
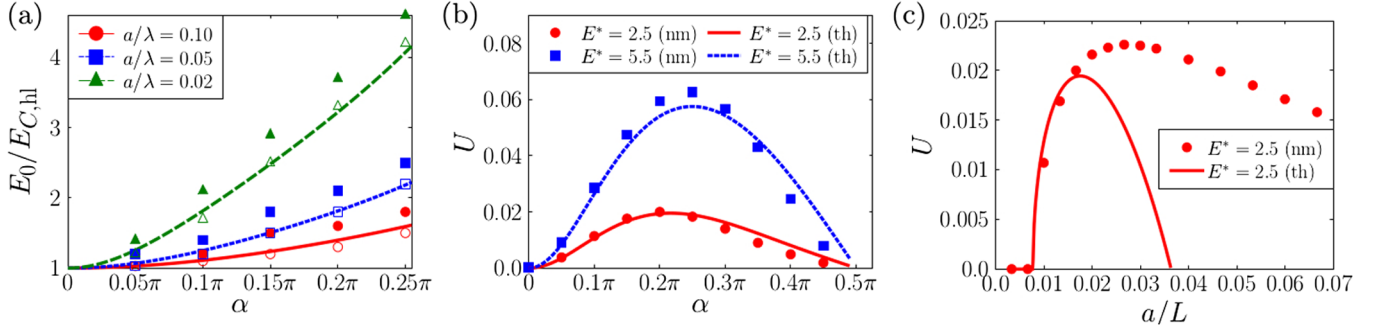
FIG. 4. (a) Critical electric field of a helix with three different cross-sectional radii but fixed number of turns, $N = 1$, plotted against the pitch angle. Red, blue, and green indicate $a/\lambda = 0.10, 0.05, 0.02$, respectively. Open and filled symbols indicate no swimming and swimming, respectively, computed using numerical simulations based on boundary element method while solid and dashed lines represent $E^*/\sqrt{1+G}$. (b) Swimming speed versus pitch angle for a helix with aspect ratio $a/L = 0.0167$ for two different electric field strengths, $E^* = 2.5$ (red circle and solid line indicate theory and simulations, respectively) and $E^* = 5.5$ (blue square and dashed line indicate theory and simulations, respectively). (c) Swimming speed versus cross-sectional radius of a helix keeping the electric field $E^* = 2.5$, number of turns $N = 3$, pitch angle $\alpha = 0.2\pi$, and pitch $\lambda/L = 0.27$ fixed (red circle and solid line indicate theory and simulations, respectively). Movies associated with (c) are available in the Supplemental Material [26].

The hydrodynamics of a helix can be described using the framework of resistive-force theory, which is valid for slender filaments moving in viscous fluids in the absence of inertia [33]. Assuming that the helix axis remains aligned with the x direction, the components of the resistance matrix relevant for the analysis below are $\mathcal{R}_{44} = LR_h^2(\zeta_\perp\cos^2\alpha + \zeta_\parallel\sin^2\alpha)$, $\mathcal{R}_{11} = L(\zeta_\parallel\cos^2\alpha + \zeta_\perp\sin^2\alpha)$, $\mathcal{R}_{14} = \chi LR_h^2\sin\alpha\cos\alpha(\zeta_\parallel - \zeta_\perp)$, and $\mathcal{R}_{13} = \mathcal{R}_{34} = 0$. All other elements of the resistance matrix are provided in the Supplemental Material [26]. Here, $\zeta_\parallel$ and $\zeta_\perp$ are the drag coefficients for local motion of the helix along the directions parallel and perpendicular to its tangent [26,34]. For the electric problem, we assume that the helix is identical to a cylinder of the same contour length, a reasonable approximation if the helix has a small pitch angle (i.e., small amplitude). The resulting electric and viscous torque acting on the helix are then given by

$$\boldsymbol{T}_E = 2\pi\varepsilon^+ a^2 L E_0^2(\boldsymbol{P} \times \boldsymbol{E}_0), \quad (7)$$

$$\boldsymbol{T}_H = -(4\pi a^2 L\Omega_1 + \mathcal{R}_{44}\Omega_1 + \mathcal{R}_{14}U_1)\hat{\boldsymbol{x}}, \quad (8)$$

where $\boldsymbol{P}$ is the effective dipole moment of the helix. Because there is no electric force acting on the particle, we have $\boldsymbol{F}_E = -\boldsymbol{F}_H = \boldsymbol{0}$, leading to a relation between translational and angular velocity

$$U_1 = -\Omega_1(\mathcal{R}_{14}/\mathcal{R}_{11}). \quad (9)$$

Balancing electric and viscous torques on the helix, $\boldsymbol{T}_E + \boldsymbol{T}_H = \boldsymbol{0}$, leads to a relation between P_2 and Ω_1

$$E^{*2}P_2/(\bar{\varepsilon}_{cl} - \bar{\sigma}_{cl}) - (1 + G)\Omega_1 = 0, \quad (10)$$

where $G = (\mathcal{R}_{44} - \mathcal{R}_{14}^2/\mathcal{R}_{11})/(4\pi\mu a^2 L)$ is a helical shape factor that only depends on geometry. The relaxation

equation of the effective dipole moment of the helix derived from the charge conservation equation, Eq. (1), provides another relation between P_2 and Ω_1 [26]

$$P_2 = (\bar{\varepsilon}_{cl} - \bar{\sigma}_{cl})\Omega_1/(1 + \Omega_1^2). \quad (11)$$

Eliminating P_2 from Eqs. (10) and (11), we obtain two solutions for the angular velocity of a helix under Quincke rotation: (i) the trivial solution, $\Omega_1 = 0$ and (ii) the steady-state rotation solution

$$\Omega_1 = \sqrt{E^{*2}/(1+G) - 1}. \quad (12)$$

The critical electric field for Quincke rotation of a helix is then given as $E_{C,hl} = E_{C,cl}\sqrt{1+G}$ while the predicted swimming speed is given by Eq. (9).

The predictions from this theoretical approach are compared with the computational results in Fig. 4. The theory is able to reproduce all features of the computational study, including the supercritical pitchfork bifurcation (at a fixed field strength) showing nonexistence of swimming states for filaments that are too slender. This is because while the electric torque on the particle scales as a^2, the viscous torque scales as $a^2 + R_h^2$; see Eqs. (7) and (8). The breakdown of the theory for large values of a/L is expected since the hydrodynamics based on resistive-force theory is accurate only in the asymptotic limit of slender filaments, $a/L \to 0$.

In summary, we have shown in this Letter that the classical Quincke rotational instability of dielectric particles under dc electric fields can lead to spontaneous self-propulsion in a bulk fluid when combined with geometrical asymmetry. The phenomenon occurs in the absence of any nearby surfaces, in stark contrast to Quincke rollers which require the presence of walls to break symmetries and

swim. While a single particle rotates and translates in a plane perpendicular to the electric field, suspensions of such particles are expected to display out-of-plane swimming resulting from three-dimensional electrohydrodynamic interactions. As a practical example, we consider a helical particle made of Polymethyl methacrylate suspended in various classical dielectric fluids and predict swimming speeds of tens of microns per second (see the Supplemental Material [26]). The physical mechanism of this new form of self-propulsion was demonstrated using numerical computations for the full system in the case of a helical filament and confirmed analytically by a theoretical approach in the slender-helix limit. Though we have focused on the special case of helical particles, self-propulsion is expected to occur for any kind of asymmetric particles whose resistance matrix, **R**, contains a nonzero off-diagonal term enabling coupling of an imposed rotation to translation. Suspensions of randomly shaped particles under Quincke rotation interacting electrohydrodynamically are thus expected to perform collective motion by exploring the full three-dimensional space, thereby opening doors to a potentially new type of active matter.

---

[*]dd496@damtp.cam.ac.uk

[†]e.lauga@damtp.cam.ac.uk

[1] T. Vicsek and A. Zafeiris, Phys. Rep. **517**, 71 (2012).

[2] M. C. Marchetti, J.-F. Joanny, S. Ramaswamy, T. B. Liverpool, J. Prost, M. Rao, and R. A. Simha, Rev. Mod. Phys. **85**, 1143 (2013).

[3] D. Saintillan, Annu. Rev. Fluid Mech. **50**, 563 (2018).

[4] T. Vicsek, A. Czirók, E. Ben-Jacob, I. Cohen, and O. Shochet, Phys. Rev. Lett. **75**, 1226 (1995).

[5] J. Toner and Y. Tu, Phys. Rev. E **58**, 4828 (1998).

[6] C. Bechinger, R. Di Leonardo, H. Löwen, C. Reichhardt, G. Volpe, and G. Volpe, Rev. Mod. Phys. **88**, 045006 (2016).

[7] W. F. Paxton, K. C. Kistler, C. C. Olmeda, A. Sen, S. K. S. Angelo, Y. Y. Cao, T. E. Mallouk, P. E. Lammert, and V. H. Crespi, J. Am. Chem. Soc. **126**, 13424 (2004).

[8] J. R. Howse, R. A. L. Jones, A. J. Ryan, T. Gough, R. Vafabakhsh, and R. Golestanian, Phys. Rev. Lett. **99**, 048102 (2007).

[9] A. Bricard, J.-B. Caussin, N. Desreumaux, O. Dauchot, and D. Bartolo, Nature (London) **503**, 95 (2013).

[10] A. Bricard, J.-B. Caussin, D. Das, C. Savoie, V. Chikkadi, K. Shitara, O. Chepizhko, F. Peruani, D. Saintillan, and D. Bartolo, Nat. Commun. **6**, 7470 (2015).

[11] A. Kaiser, A. Snezhko, and I. S. Aranson, Sci. Adv. **3**, e1601469 (2017).

[12] J. Palacci, S. Sacanna, A. P. Steinberg, D. J. Pine, and P. M. Chaikin, Science **339**, 936 (2013).

[13] Z. Izri, M. N. van der Linden, S. Michelin, and O. Dauchot, Phys. Rev. Lett. **113**, 248302 (2014).

[14] S. Thutupalli, R. Seemann, and S. Herminghaus, New J. Phys. **13**, 073021 (2011).

[15] G. Quincke, Ann. Phys. Chem. **295**, 417 (1896).

[16] P. F. Salipante and P. M. Vlahovska, Phys. Fluids **22**, 112110 (2010).

[17] D. Das and D. Saintillan, Phys. Rev. E **87**, 043014 (2013).

[18] D. Das and D. Saintillan, J. Fluid Mech. **829**, 127 (2017).

[19] J. R. Melcher and G. I. Taylor, Annu. Rev. Fluid Mech. **1**, 111 (1969).

[20] L. D. Landau, L. P. Pitaevskiì, and E. M. Lifshitz, *Electrodynamics of Continuous Media* (Pergamon Press, New York, 1984), 2nd ed..

[21] L. Zhang, J. J. Abbott, L. Dong, B. E. Kratochvil, D. Bell, and B. J. Nelson, Appl. Phys. Lett. **94**, 064107 (2009).

[22] A. Ghosh and P. Fischer, Nano Lett. **9**, 2243 (2009).

[23] E. Lauga, Annu. Rev. Fluid Mech. **48**, 105 (2016).

[24] C. Pozrikidis, *A Practical Guide to Boundary Element Methods with the Software Library BEMLIB* (Chapman & Hall/CRC, Boca Raton, 2002).

[25] C. Pozrikidis, *Introduction to Theoretical and Computational Fluid Dynamics* (Oxford University Press, New York, 2011).

[26] See Supplemental Material at http://link.aps.org/supplemental/10.1103/PhysRevLett.122.194503 for a full description of the numerical method and its validation, hydrodynamic resistance matrix of a helix, discussion on swimming speeds of a helix under Quincke rotation achievable in experiments, and movies of a cylinder and helices under Quincke rotation, which includes Refs. [27–31].

[27] D. Das and D. Saintillan, J. Fluid Mech. **810**, 225 (2017).

[28] H. C. Fu, M. Jabbarzadeh, and F. Meshkati, Phys. Rev. E **91**, 043011 (2015).

[29] N. Pannacci, L. Lobry, and E. Lemaire, Phys. Rev. Lett. **99**, 094503 (2007).

[30] N. Pannacci, E. Lemaire, and L. Lobry, Eur. Phys. J. E **28**, 411 (2009).

[31] S. Q. Lu, B. Y. Zhang, Z. C. Zhang, Y. Shi, and T. H. Zhang, Soft Matter **14**, 5092 (2018).

[32] T. B. Jones, *Electromechanics of Particles* (Cambridge University Press, Cambridge, United Kingdom, 2005).

[33] E. Lauga and T. R. Powers, Rep. Prog. Phys. **72**, 096601 (2009).

[34] J. Lighthill, SIAM Rev. **18**, 161 (1976).